Australian National University
Crawford School of Public Policy

CAMA

Centre for Applied Macroeconomic Analysis

Impacts from Autonomous EV Travel over Personal Aviation in Europe

CAMA Working Paper 90/2025
October 2026

Anthony Wiskich
Centre for Applied Macroeconomic Analysis, ANU
Swinburne University of Technology

Abstract

Autonomous and electric vehicles could shift personal travel from aviation to roads, changing a basket of external costs – climate, accidents, noise, air pollution and land. We estimate the effect for European personal travel with a parsimonious discrete-choice model of car, rail and air, whose substitution elasticity sets a nonlinear "modal cliff" – the car-to-air switch as distance rises – estimated on European modal splits. Re-parameterising the car for a mature autonomous electric fleet draws travellers from both aviation and rail: personal air passengers on land-connected routes fall by a quarter (24.6% centrally, 18% to 32% across plausible distaste for driving, the key uncertainty). Because emissions concentrate in longer flights cars cannot replace, the shift reaches about a fifth (19%) of land-connected aviation CO_2e and cuts its external cost by as much: with an electric fleet a switched flight's warming is avoided almost in full, and short-haul switchers shed disproportionate noise and air-pollution costs. Automation neutralises driving's accident cost and electrification its climate cost, more than halving driving's external cost from 5.1ct/pkm to 2.2ct/pkm at a conservative 100€ per tonne CO_2.

Keywords

aviation, autonomous vehicles, rail, modal substitution, external costs, discrete choice

JEL Classification

O33, Q54, R40, R41

Address for correspondence:

(E) cama.admin@anu.edu.au

ISSN 2206-0332

The Centre for Applied Macroeconomic Analysis in the Crawford School of Public Policy has been established to build strong links between professional macroeconomists. It provides a forum for quality macroeconomic research and discussion of policy issues between academia, government and the private sector.

The Crawford School of Public Policy is the Australian National University's public policy school, serving and influencing Australia, Asia and the Pacific through advanced policy research, graduate and executive education, and policy impact.

Impacts from autonomous EV travel over personal aviation in Europe

Anthony Wiskich*

This draft: September 26, 2026

Abstract

Autonomous and electric vehicles could shift personal travel from aviation to roads, changing a basket of external costs – climate, accidents, noise, air pollution and land. We estimate the effect for European *personal* travel with a parsimonious discrete-choice model of car, rail and air, whose substitution elasticity sets a nonlinear "modal cliff" – the car-to-air switch as distance rises – estimated on European modal splits. Re-parameterising the car for a mature autonomous electric fleet draws travellers from both aviation and rail: personal air passengers on land-connected routes fall by a quarter (24.6 % centrally, 18 % to 32 % across plausible distaste for driving, the key uncertainty). Because emissions concentrate in longer flights cars cannot replace, the shift reaches about a fifth (19 %) of land-connected aviation CO_2e and cuts its external cost by as much: with an electric fleet a switched flight's warming is avoided almost in full, and short-haul switchers shed disproportionate noise and air-pollution costs. Automation neutralises driving's accident cost and electrification its climate cost, more than halving driving's external cost from 5.1 ct/pkm to 2.2 ct/pkm at a conservative 100 € per tonne CO_2.

JEL: O33, Q54, R40, R41. **Keywords:** aviation; autonomous vehicles; rail; modal substitution; external costs; discrete choice.

1 Introduction

Aviation is one of the hardest transport sectors to decarbonise. It is a growing share of transport emissions, its warming effect is amplified by non-CO_2 impacts at altitude, and its

*Centre for Applied Macroeconomic Analysis, Crawford School of Public Policy, Australian National University; and School of Business, Law & Entrepreneurship, Swinburne University of Technology. Email: tony.wiskich@anu.edu.au.

main mitigation levers – sustainable aviation fuels (SAF) and efficiency – are slow and costly to deploy (Lee et al., 2021; EASA and EEA and EUROCONTROL, 2022). European policy has responded with the aviation Emissions Trading System and the ReFuelEU sustainable-fuel mandate (European Union, 2023, 2009), to encourage a switch to cleaner fuels.

A second, demand-side channel is essentially absent from aviation's decarbonisation ledger. The levers above – the ETS and ReFuelEU – and the net-zero pathways built on them are supply-side, turning on cleaner fuels and more efficient aircraft; while demand-side responses are considered, such as reduced long-haul business flights in the IEA's net-zero roadmap, road substitution is not (International Energy Agency, 2023). Vehicle automation is expected to lower the perceived cost of driving by freeing the driver's time, and electrification lowers its running cost; together they could divert travellers from planes (and from trains) onto roads (Singleton, 2019; Wadud et al., 2016). The handful of studies that model autonomous-vehicle competition with aviation find large but widely varying diversion, from around 47 % to over 80 % on short corridors, depending on the assumed cost and time savings (Perrine et al., 2020; LaMondia et al., 2016; Gurumurthy and Kockelman, 2020). What these studies do not do is value the shift: a traveller moved from a plane to a car changes not only CO_2e but the wider basket of external costs – accidents, noise, local air pollution, congestion and land-take – quantified for Europe in the external-cost handbooks used for transport appraisal (van Essen et al., 2019a,b). In Europe the accounting is further complicated by rail: on many corridors the train, not the plane, is the cleanest option, so an improvement to driving that pulls travellers off rail can *raise* social costs even as it lowers them elsewhere (Dobruszkes, 2011).

This paper quantifies both sides of that ledger for European *personal* travel. We focus on personal trips – leisure and visiting friends and relatives, excluding business (about a quarter of European air trips), as we are less confident that our model structure is appropriate for business travel.

We make two contributions. The first is the estimated model: a deliberately parsimonious, representative-consumer disutility model in which car, rail and air compete through a constant elasticity of substitution (CES) with multiplicative Fréchet errors (Anderson et al., 1992; Eaton and Kortum, 2002). That single elasticity sets the non-linear "modal cliff" – the sharp switch from car to air as trip distance rises (Thrane, 2015) – so a small improvement to the car can trigger a large air-to-car shift over a band of intermediate distances. We *estimate* the identified structural core – the substitution elasticity, the value of travel time, the must-drive share and two rail constants – on European personal modal splits, and the framework is portable.

The second contribution is the impact analysis: we put a number on a lever the decar-

bonisation literature currently values at zero – the emissions and welfare effect of a mature, near-universal fleet of autonomous EVs, including a small contribution from overnight robotaxis, holding aggregate travel fixed. We ask how much of aviation's *climate* burden road substitution can actually reach, how that effect falls unevenly across routes and airports, and what the shift is worth in emissions and *social* terms.

We find that this uncounted lever delivers a material climate dividend. On land-connected routes roughly a quarter of personal air passengers switch to cars under this scenario, and the shift reaches about a fifth of the land-connected personal aviation CO_2e it can reach in Europe – obtained *without* any carbon price or fuel-mandate cost in the projection, induced purely by the cheaper, time-freeing car riding a fleet transition already under way for unrelated reasons. The dividend concentrates on the shortest, lowest-emission trips, which is what caps it at a fifth rather than the full behavioural response. The response is steeply distance-graded: cars take about two-thirds of personal air passengers on the shortest corridors (under 500 km – for instance 66 % on Barcelona–Madrid, the largest such route) but under a twentieth beyond 1500 km (about 3 % on Frankfurt–Istanbul), so trips shorter than 1000 km account for roughly five-sixths of the avoided CO_2e. The magnitude of this response scales with how strongly travellers dislike driving (γ), a parameter we transfer rather than estimate and vary in sensitivities.

We value the shift as an equilibrium reallocation across car, rail and air – not a simple air-to-car swap – on three levels. First, at the system level: the land-connected personal aviation the car can reach imposes about 10.8 bn € a year in external costs, and the shift removes about a fifth of that – roughly 2.1 bn (from 10.8 to 8.7 bn € a year; Figure 3a). That cost cut matches the fifth of CO_2e the shift delivers, because the incoming electric fleet avoids a switched flight's warming almost in full. Second, the incoming car is far cleaner per kilometre: electrification and automation more than halve driving's own external cost, from about 5.1 ct/pkm to 2.2 ct/pkm, as electrification removes the climate cost (the single largest item) and automation almost eliminates the accident cost. Third, netting the added road noise, land-take and congestion and the rail-to-car leakage against the avoided flight leaves only a modest saving per switching trip – the external cost of a switch falls from about 24 € to 18 € (roughly 1 ct/pkm). This net is the smallest and most fragile figure: it is a net *cost* for the roughly 55 % of switchers who travel alone, and it turns on the carbon price and how quickly aviation decarbonises (Section 5.3).

2 Model

We adapt the disutility framework of Wiskich (2026) extended from two modes to three. Disutility per traveller for mode m on trip n is $U_{m,n} = V_{m,j,N}(\boldsymbol{\beta})\,\varepsilon_{m,n}(\sigma)$, where a higher U is worse, $V_{m,j,N}$ is the deterministic disutility (generalised cost) for mode m on route j with party size N, and ε is a multiplicative Fréchet error whose shape parameter σ is the elasticity of substitution of a representative-consumer CES utility (Anderson et al., 1992).

2.1 Deterministic disutilities

Car. Driving distance δ_j and duration τ_j are taken directly from road routing (Section 3), so τ_j reflects the actual road network – motorway versus mountain or fjord detour – rather than a flat assumed speed. The value of travel time (VTT) χ is common to all three modes; for the car the driver's VTT carries an uplift $\gamma > 1$, variable cost per km is π, and costs are shared across the party of size N:

$$V_{c,j,N} = \frac{\tau_j\,\chi\,(\gamma + N - 1) + \delta_j\,\pi}{N}. \tag{1}$$

The variable cost $\pi = 0.16\,€$/km is the perceived marginal cost of driving in Europe: at a pump price of $\sim$1.75 € per litre and $\sim$6.5 L per 100 km, fuel alone is $\sim$0.11 €/km, and adding variable wear (tyres, part of maintenance) recovers this figure.

Air. For great-circle distance Δ_j, a route-specific detour correction DC_j (the extra distance from the empirical detour factor of Section 3) gives flown distance $\Delta_j + DC_j$ and, at cruise speed S, cruise time $T_j = (\Delta_j + DC_j)/S$. A fixed time Γ captures access, airport and take-off/landing time; Ψ is a per-airport, per-party financial access cost, so both endpoints contribute 2Ψ. The one-way fare splits into a fixed component Φ and a variable component Υ on distance beyond 500 km, uplifted by Ω to average prices. Of the quantities in the three deterministic disutilities, only the value of travel time χ is estimated on the European data (Section 4); the fares, engineering and access constants, and the transferred car parameters (γ, π), are calibrated to external data and collected in Appendix A. The air disutility is:

$$V_{a,j,N} = \frac{2\Psi + N\big(\Omega\big(\Phi + \Upsilon\max(0, \Delta_j - 500)\big) + \chi(T_j + \Gamma)\big)}{N} + A_j. \tag{2}$$

Below 500 km the fare is thus a floor $\Omega\Phi$ (about 62 € at European yields, the value of the fitted yield line at the 500 km kink where the distance-variable term switches on). Short-haul tickets do not fall in proportion to distance once taxes, fees and minimum operating

costs are counted; a linear-from-origin fare would price very short flights implausibly low and over-state short-haul air's attractiveness. The final term A_j collects the reduced-form air alternative-specific constants (ASCs) that shift a corridor's baseline air level to absorb systematic modal preferences the generalised cost omits:

$$A_j = \mathrm{ASC}^{\mathrm{ctry}}_{o(j)} + \mathrm{ASC}^{\mathrm{ctry}}_{d(j)} + \mathrm{ASC}_{\mathrm{intl}}\,\mathbf{1}\{j \text{ cross-border}\} + \mathrm{ASC}_{\mathrm{feeder}}\,\omega_j, \tag{3}$$

an additive constant for each endpoint country ($o(j)$ and $d(j)$ index route j's origin and destination country), an international constant for cross-border routes, and a nuisance constant on the connection-feeder routes weighted by $\omega_j \in [0,1]$ – a graded feeder weight (a logistic in observed air share on eligible hub corridors; Section 4) that scales the pivot continuously from genuine ($\omega_j = 0$) to near-certain feeder ($\omega_j = 1$) rather than a hard switch. These are estimated jointly with the structural parameters (Section 4); being level shifts rather than behavioural parameters, they move a route's baseline air share but not its response to the scenario levers.

Rail. Rail in-vehicle time, frequency and user cost come directly from the ETISplus network model (Section 3); only where a route lacks them do we fall back to a network detour factor on the great-circle distance at an average operating speed. The observed rail generalised cost enters as:

$$V_{r,j,N} = \mathrm{fare}_j + \chi\big(T_{r,j} + a_r + w(f_j)\big) + \mathrm{ASC}_{s(j)}, \qquad s(j) \in \{\mathrm{HSR},\ \mathrm{conv}\}, \tag{4}$$

where $T_{r,j}$ is in-vehicle time, a_r a fixed access time, $w(f_j) = \min\big(\bar{w},\, H/(2f_j)\big)$ the expected wait – half the mean headway over an $H = 16\,\mathrm{h}$ service window, capped at $\bar{w} = 3\,\mathrm{h}$ – given daily frequency f_j, fare_j the observed user cost, and $\mathrm{ASC}_{s(j)}$ a rail alternative-specific constant taking one of two estimated values – $\mathrm{ASC}_{\mathrm{HSR}}$ if corridor j is served by high-speed rail and $\mathrm{ASC}_{\mathrm{conv}}$ otherwise (the two are estimated jointly; Section 4).

2.2 Choice probabilities

With multiplicative Fréchet errors, a constant "must-drive" share θ is committed to the car – allowing a long-distance tail of car travel that no price or time change reallocates – and the remaining $(1-\theta)$ of travellers split across the three modes by CES:

$$p_{a,j,N} = (1-\theta)\frac{V_{a,j,N}^{-\sigma_j}}{D_j}, \quad p_{r,j,N} = (1-\theta)\frac{V_{r,j,N}^{-\sigma_j}}{D_j}, \quad p_{c,j,N} = \theta + (1-\theta)\frac{V_{c,j,N}^{-\sigma_j}}{D_j}, \tag{5}$$

where $D_j = \sum_k V_{k,j,N}^{-\sigma_j}$ over $k \in \{\text{car}, \text{rail}, \text{air}\}$. By construction the three shares sum to one: the car receives both its CES share and the must-drive residual θ, so (5) generalises the two-mode logit while remaining a proper modal split. Aggregate shares are the party-size–weighted average of (5) over the party-size mix.

The elasticity is *route-specific*: substitution is soft on drivable corridors, where the car is a genuine option, and near-deterministic on long-haul routes, where almost everyone flies. We therefore let σ_j depend on the route's car drive time τ_j (Eq. 1) through two estimated regime values, σ_{short} (drivable) and σ_{long} (long-haul), joined by a continuous linear ramp so that predicted shares do not jump where a route crosses the boundary:

$$\sigma_j = \sigma(\tau_j) = \begin{cases} \sigma_{\text{short}}, & \tau_j \le \bar{\tau} - w, \\ \sigma_{\text{short}} + \left(\sigma_{\text{long}} - \sigma_{\text{short}}\right) \dfrac{\tau_j - \bar{\tau} + w}{2w}, & \bar{\tau} - w < \tau_j < \bar{\tau} + w, \\ \sigma_{\text{long}}, & \tau_j \ge \bar{\tau} + w, \end{cases} \tag{6}$$

with a profiled regime midpoint $\bar{\tau} \approx 15\,\text{h}$ and half-width $w = 2\,\text{h}$ (Section 4). Both regime elasticities are estimated; the transition band falls where air share is already about 0.9, so it is σ_{short} that governs the modal cliff and the autonomy response, while σ_{long} only sharpens the saturated long-haul plateau. A single pooled elasticity ($\sigma_j \equiv \sigma$) is the special case reported as a robustness row (Section 5.4).

2.3 Scenario levers

The base case reproduces observed 2019 shares. A future autonomous-vehicle (AV) world is represented by adjusting the *car* option through composable levers, so that substitution flows to cars from both aviation and rail:

- **av** – autonomy removes the driver VTT uplift ($\gamma \to 1$) (Singleton, 2019).
- **ev** – electrification lowers the car's variable running cost by about 0.09 €/km (from 0.16 €/km to about 0.07 €/km).
- **on** – an overnight option values a minimum eight-hour sleep window at half the VTT (waking hours beyond it at the full rate) for a small running-cost uplift (about 0.12 €/km); it is offered to the 50 % of travellers assumed to consider sleeping en route, each taking it only where it beats the daytime drive.
- **spd** – higher car speed enabled by improved safety.
- **tax** – a carbon price on aviation fuel, raising fares.

The overnight option modifies the car disutility of Eq. (1). In the autonomous world the driver uplift is gone ($\gamma \to 1$), so the daytime time cost collapses to $\tau_j\,\chi$; the overnight variant instead values a fixed sleep window $H = 8\,\text{h}$ at a reduced rate $\phi_s\chi$ (with $\phi_s = 0.5$) and only the waking excess $(\tau_j - H)_+$ at the full rate, for a running-cost uplift $\kappa \approx 0.12\,€/\text{km}$ on the electric running cost π_{ev}:

$$V^{\text{on}}_{c,j,N} = \phi_s\,\chi\,H + \chi\,(\tau_j - H)_+ + \frac{\delta_j\,(\pi_{\text{ev}} + \kappa)}{N}, \tag{7}$$

where $(x)_+ = \max(0, x)$. A traveller offered the option takes $\min\big(V^{\text{on}}_{c,j,N},\, V_{c,j,N}\big)$, so it can never make them worse off, and only a share $s_{\text{on}} = 0.5$ of travellers consider it; the route's predicted shares are the corresponding s_{on}-weighted mixture of the two. Our *headline* scenario, "AVcore", bundles {av, ev, on}. Overnight travel is included in the headline because it depends on technology we expect to mature (a vehicle able to drive safely while its occupants sleep is a direct consequence of full automation and safer roads), whereas higher car speed is held out as a separate increment because it depends on a change to motorway speed limits – a policy choice, not a technological one, outside the few jurisdictions with unrestricted sections. The aviation carbon price (absent in 2019) is likewise a policy increment. The carbon-price and sustainable-fuel levers are EU policy instruments binding on the EU/EEA subset of the network; we read their sensitivities as the effect of EU-style policy spreading across European aviation.

2.4 Valuing the shift: net external cost

The AV levers pull travellers to cars from *both* aviation and rail. We value this as a comparison of the base and AVcore modal splits on each route:

$$\text{net saving} = (\text{air lost})\,(C_{\text{air}} - C_{\text{car}}) + (\text{rail lost})\,(C_{\text{rail}} - C_{\text{car}}), \tag{8}$$

where C_m is the per-trip external cost of mode m (per-km external cost times leg distance, plus access). Air-to-car substitution saves aviation's large climate cost; rail-to-car substitution is a social *cost*, a clean train replaced by a car. Under AVcore the substitute car is electric and automated (lower accident, air-pollution and climate externalities) and rail is further decarbonised – its traction climate and well-to-tank (WTT) costs cut, though by less than the car's because most European rail is already electric, with its non-traction externalities (accidents, noise, land-take) unchanged; aviation follows a decarbonisation dial whose base is a modest efficiency gain on 2019. Each mode's external-cost categories are scaled by fixed factors relative to 2019; these are collected in the lower block of Table 7, with the

aviation factors flexed in the lower block of Table 5. An *ICE-today* (internal-combustion-engine) valuation of the same switching at 2019 technology isolates how much the benefit depends on a clean (and safer) ground fleet. We report the net effect per switching trip and per passenger-kilometre – our preferred, assumption-light normalisation – and also as an aggregate euro-per-year total; the aggregate scales the per-trip figure by all 93 million switchers and so presumes a mature, near-universal autonomous-electric fleet. Aviation's external cost is split into per-km cruise costs (climate – CO_2 plus a non-CO_2 warming multiplier that captures contrail and NO_x forcing – and WTT) and per-flight landing/take-off (LTO) costs (noise, local air pollution, accidents), so that short flights correctly carry a higher per-passenger-kilometre cost.

3 Data

Scope: personal travel. ETISplus classifies trips by purpose – Business, Private (up to four days), Vacation (over four days) and Commuting. We define *personal* travel as Private + Vacation, which make up 73 % of European air travel.

Party size. The car option shares its per-vehicle costs (fuel, tolls, and the driver's time penalty) over the travelling party, so party size shifts the car–air balance. We assume a persons-weighted mix over $N = 1, 2, 3, 4$ of 0.45, 0.30, 0.10 and 0.15 (solo travellers the largest single group, then couples); the multi-person split follows the long-distance leisure/visiting-friends-and-relatives (VFR) party-size shares of Outwater et al. (2015). The mix is a transferred assumption – the aggregate European flows do not identify it – and Section 5.4 shows the headline is robust to plausible re-weightings (the re-estimated value of travel time absorbs the change). Aggregate modal shares are the party-size-weighted average of the route-level choice probabilities. The structural parameters are estimated by maximum likelihood on the European personal modal splits; the method and identification tiers are set out in Section 4 and Appendix A.

Aviation demand and geographic scope. Passenger volumes are 2019 Eurostat air passenger statistics (`avia_par`), scaled to personal air by each route's personal fraction. Our denominator is *personal intra-European* aviation – flights with both endpoints in the Eurocontrol European area (EU27, EFTA, the UK, the Western Balkans, Ukraine, Moldova and Turkey; Russia excluded). This is 598 million personal passengers and, by our estimate, 164 Mt CO_2e. The CO_2e figure applies distance-banded CO_2 intensities (about 0.10 kg/pkm to 0.19 kg/pkm, highest on the short, landing/take-off–heavy hops; the intensity bands, listed

in Appendix A, are finer than the four reporting bands of Table 1) to flown, detour-corrected passenger-kilometres, then multiplies by a non-CO_2 warming factor of 2.0 to include contrail and NO_x forcing; its sensitivity to that factor and to its distance profile is examined in Table 4. Table 1 shows how these split by distance: short flights are a large share of passengers but a small share of emissions, which (as Section 5 shows) is what bounds the climate payoff of mode shift.

Table 1: Passengers versus CO_2e by great-circle distance band, over all intra-European aviation (2019) – the full 598-million-passenger denominator, not the modelled land-connected subset.

Band (km)	Routes	Passengers (%)	CO_2e (%)
0–500	650	20.9	11.3
500–1000	1337	31.0	22.4
1000–2000	2191	35.9	42.3
2000+	920	12.2	23.9

Flown distance, driving, rail. Flown air distance exceeds the great-circle distance because of routing, holding and terminal-area manoeuvring. We capture this with an empirical detour factor from the GAIA global flight inventory (Teoh et al., 2024): a route's own flown/great-circle ratio where available (about 88 % of land-connected routes, carrying 95 % of their air passengers) and otherwise a fitted curve (Appendix A), so the detour ratio falls from about 1.13 on short hops to 1.03 on long ones. This flown distance feeds both air time and aviation emissions. Driving distances and times come from routing data (Luxen and Vetter, 2011), retaining routed *times* so that ferries and fjord detours are captured; rail in-vehicle time, frequency and user cost come from the ETISplus network model (base year 2010) (ETISplus Consortium, 2013). ETISplus is the last freely available pan-European, NUTS-3, multimodal origin–destination matrix carrying a mode split; its successor TRIMODE (base year 2015) is not released publicly at this granularity, and Eurostat's up-to-date modal split is national aggregate passenger-kilometres without origin–destination structure. Air *demand* is therefore 2019 throughout; only the ground network and modal split are 2010.

External costs. Per-passenger-kilometre external costs by category are from the CE Delft handbook (van Essen et al., 2019a): motorway values for the line-haul car leg, all-roads values for access, an occupancy correction for the party mix, and scaling of the future car and rail options for electrification and automation.

Coverage. A route is "land-connected" if a road path exists between its endpoints. Of the land-connected airport pairs with a road path, about sixty lack an ETISplus modal split altogether and are dropped (about 3 % of land-connected air; distinct from the connection-feeder routes, which have data but inflated air, retained in Section 4), leaving 2694 modelled; excluding the twelve connection-trunk routes (Section 4) leaves 2682 reported routes. These carry 339 million personal air passengers, 57 % of personal intra-European passengers (their smaller CO_2e share, and what it implies, are taken up in Section 5). Estimation and validation collapse airport pairs that map to a single ETISplus zone pair to 2451 representative routes, since such pairs share one observed modal split and are not independent observations (Section 4). The collapse concerns the *observation*, not passengers – each airport pair keeps its own Eurostat volume and the representative carries the group's summed air traffic – so the headline shift is reported over the full 2682, letting every airport pair enter the counterfactual with its own driving, rail and detour geometry.

4 Estimation and validation

4.1 Estimation

We estimate the identifiable structural parameters – the elasticity of substitution, the value of travel time χ, the must-drive share θ, and two rail alternative-specific constants (ASC_{HSR} for high-speed corridors and ASC_{conv} for conventional rail) – on European personal modal splits by maximum likelihood, with no priors. We let the substitution elasticity differ between two drive-time regimes – a *drivable* regime with elasticity σ_{short} and a *long-haul* regime with σ_{long}, all other parameters common – because a single elasticity is pulled upward by the near-deterministic long-haul routes and over-states substitution on the drivable corridors the counterfactual actually reaches (the continuous ramp of Eq. (6), with a profiled midpoint $\bar{\tau} \approx 15\,\text{h}$ and half-width 2 h). Both regime elasticities are estimated; a single-elasticity fit is one row of the robustness table (Section 5.4). Identification runs in three tiers. We *estimate* the structural parameters that aggregate route-level modal shares can support (together with the reduced-form country, international and connection-feeder air constants described below). We *transfer* the party-size behavioural structure that aggregate flows cannot identify – the driver VTT uplift ($\gamma = 1.69$, Wiskich, 2026) and the party-size mix (Outwater et al., 2015). Section 5.4 shows the headline is robust to the assumed party mix but scales with the driver VTT uplift γ. We *calibrate* the remaining inputs to external data – the air fare to observed European yields, engineering constants (cruise speed, routing detour, fixed airport and access times), road tolls, and the external-cost layer; these calibrated inputs, with their

sources, are collected in Appendix A. The air fare uses a single Europe-wide yield curve.

Two features of the estimation sample matter. First, we handle connection-inflated routes – whose observed air is swollen by onward-connecting passengers Eurostat records on the segment but ETISplus ground data do not (Appendix C) – in three groups by the strength of the signal. *Trunk* routes between two of the twenty largest airports (12 routes, 2.2 % of land-connected air) are so dominated by connecting traffic that no genuine point-to-point market our framework describes remains; we exclude them from both estimation and the reported results. *Feeder* routes – a single large-airport endpoint, near-total observed air, and a feasible ground alternative, a short drive *or* frequent rail (59 routes, 5.9 %) – are part genuine and part connecting and cannot be cleanly separated; rather than discard them we keep them with one nuisance air alternative-specific constant, estimated jointly (a large air discount of about -130 €). This both stops their contamination from distorting the structural parameters *and*, carried into the forward model, pivots them toward their observed high-air base so they receive a realistic response rather than the full modal-cliff shift (Appendix B). The pivot is applied with a *graded* weight ω_j rather than an all-or-nothing switch, so that two near-identical corridors just either side of the cut are not treated discontinuously. A corridor is eligible for the pivot if it has a single top-20 hub endpoint, a great-circle distance below 700 km, and a feasible ground alternative – a drive under 6 h *or* frequent rail. On that eligible set the weight is a logistic in the route's observed air share a_j,

$$\omega_j = \left[\,1 + \exp(-20\,(a_j - 0.90))\right]^{-1}, \qquad \omega_j = 0 \text{ off the eligible set,} \tag{9}$$

so the 90 % figure is the logistic's *midpoint*, not a hard cut: an eligible feeder just below it still receives a small positive weight rather than dropping to zero, and one just above receives most of the pivot. The weight thus scales the nuisance constant continuously from near-zero (a genuine route) to near-one (a near-certain feeder). All remaining routes – including genuinely high-air, poor-ground corridors such as the long Anatolian and Norwegian-fjord routes – take the full model. Second, airport pairs that map to the same ETISplus NUTS-3 zone (and so share an observed modal split) are collapsed to one representative, so multi-airport regions are not double-weighted.

Beyond the structural parameters we add a reduced-form block of route-level air alternative-specific constants that capture national and cross-border modal preferences the generalised cost omits: an endpoint-additive constant for each country with at least twenty route appearances (thirty-two countries; smaller countries absorbed in the baseline) and a single international constant separating cross-border from domestic routes. These are *not* structural – they are level shifts on the air disutility, estimated jointly with the structural parameters,

that soak up systematic corridor heterogeneity the single cost index cannot: countries whose travellers fly *less* than the cost predicts (Iberia, the Nordics and Greece, with strong domestic rail or peninsular geography) against those who fly *more* (the central-European short-hop countries), and a cross-border effect (international routes fly more than domestic at the same generalised cost). Adding them tightens the fit materially – the passenger-weighted air-share mean absolute error (MAE) on genuine routes falls from 0.111 to 0.093 and the cross-route air correlation rises from 0.76 to 0.82 – while leaving the structural core essentially unchanged, so they sharpen the description of *where* substitution happens without disturbing the behavioural parameters that govern *how much*. A purely structural specification without them is one row of the robustness table (Section 5.4, Table 6). We motivate this block – and show that a route-level barrier proxy and road tolls do *not* substitute for it – in the same section.

The likelihood is a passenger-weighted multinomial over the observed car/rail/air shares, the predicted shares being the party-mix average of the route-level probabilities (5); standard errors are from a nonparametric bootstrap over routes. We impose no priors and no regularisation: the structural parameters are well identified by the aggregate splits, and the thirty-two country constants need no ridge – estimated as unpenalised fixed effects they stay within $[-33, +74]$ € with the genuine-route air MAE unchanged. To avoid confounding model error with post-2010 demand growth, the target is a vintage-consistent benchmark (2019 air volumes with the 2010 ground network; the splice is detailed in Appendix C), and we hold out 30 % of routes to check fit (held-out air-share MAE of 0.10).

Table 2 reports the estimates. Monetary parameters are estimated on European data and reported in euros; because the choice probabilities depend only on *ratios* of disutilities, the currency scale does not affect the modal shares. The estimates describe European personal travel on their own terms: a modal-cliff elasticity of $\sigma_{\text{short}} \approx 3.3$ on drivable routes, sharpening to $\sigma_{\text{long}} \approx 5.4$ on the long-haul plateau, a leisure value of travel time of 16.8 €/h, a very small must-drive share ($\theta = 0.015$), and large rail constants – higher for conventional than high-speed rail, both consistent with leisure travellers using rail far less than the generalised cost alone would predict. Reassuringly, the companion Australian two-mode car–air model (Wiskich, 2026) estimates a single elasticity ($\sigma = 3.87$) that sits between our two regime values and is close to our own pooled-elasticity fit ($\sigma = 4.16$, the single-σ robustness row); that model has a leisure value of travel time of 19.8 €/h and a larger must-drive share ($\theta = 0.10$–0.17).

Table 2: Estimated structural parameters (European personal travel, unpenalised maximum likelihood). Monetary values in euros. Standard errors are from a 200-replication route bootstrap.

Parameter	Estimate	SE
σ_{short} (drivable elasticity)	3.29	0.17
σ_{long} (long-haul elasticity)	5.44	0.23
$\bar{\tau}$ (regime midpoint, drive h)	15	(profiled)
χ (VTT, €/h)	16.8	1.0
θ (must-drive)	0.015	0.002
ASC_{HSR} (high-speed rail, €)	110.9	8.5
ASC_{conv} (conventional rail, €)	153.9	7.1
ASC_{intl} (international air, €)	−40.9	6.2
Country air ASCs (32 countries, €)	−33 to +74	–
$\text{ASC}_{\text{feeder}}$ (connection nuisance, €)	−129.9	6.7

4.2 Validation

Table 3 compares predicted and observed personal mode shares over the full estimation sample (genuine plus feeder routes). All three statistics – correlation, bias, and MAE – are passenger-weighted, so the table is on a single consistent basis (weighting each route by its traffic, as one cares more about the fit on busy corridors). The air MAE here (0.086) includes the feeders pivoted to their observed base and so sits just below the 0.093 on genuine routes alone (Table 6); a 30 % route hold-out gives 0.10 (Section 4). The model reproduces the cross-route pattern of all three modes with small biases; rail, a tiny personal share, is essentially unbiased. The air correlation (0.84) is high: the structural parameters capture the distance and service-quality gradients that drive the aggregate result, and the country/international air constants absorb much of the residual corridor heterogeneity a single cost index leaves behind (Section 5.4 quantifies the gain). Appendix C shows the predicted-versus-observed scatter (Figure 4), the air-share gradient against distance and against the model's own cost index (Figure 5, panels (a) and (b); the former also drawn per party size $N = 1 \dots 4$), and discusses where the model misses.

5 Results

5.1 Modal shift

Under AVcore – with all three modes competing – personal air passengers fall by 24.6 %. Rail barely dampens this: removing rail as an option lifts the reduction only to 25.1 %,

Table 3: Personal modal-share validation against ETISplus (the 2439 of the 2451 representative routes – after collapsing multi-airport regions that share one ETISplus zone and excluding the 12 connection-trunk routes (Section 4) – that carry an ETISplus modal-split benchmark; vintage-corrected). Correlation, bias and MAE are all passenger-weighted.

Mode	Observed mean	Correlation	Bias (pax-wt.)	MAE
Air	0.834	0.843	−0.002	0.086
Rail	0.019	0.661	+0.002	0.015
Car	0.147	0.818	+0.000	0.079

because personal travellers use rail little to begin with. Two further levers stack on top of the headline (Figure 1a). An aviation carbon price – set at the 100 € per tonne CO_2 social cost of carbon used to value climate damages (Section 5.3), added to the fare with the same non-CO_2 uplift, so the carbon price and the carbon value are one figure – raises the shift to 30.9 %; a further 10 km/h car-speed uplift on the 90 km/h baseline, enabled by improved automated-driving safety, lifts it to 35.8 % on top of that. Speed enters only as a top-of-stack increment.

Figure 1 decomposes the shift. Panel (a) shows the cumulative lever bundles by distance: a modal "cliff" that decays with distance, with autonomy the dominant single increment (electrification alone moves far fewer travellers than electrification plus autonomy). Panel (b) shows the most-affected routes – Turkish, Iberian and dense German and Norwegian corridors – as base and post-AVcore air volumes, and panel (c) the most-affected airports (the Istanbul and Central-European hubs and the Iberian and Norwegian gateways); the full route- and airport-level rankings are in Appendix D. Figure 2 maps the network, with line colour showing the AVcore reduction.

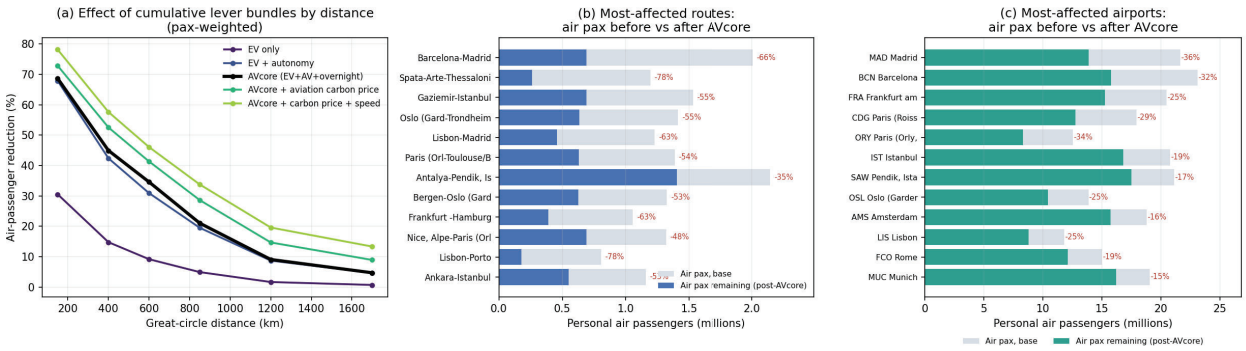


Figure 1: (a) Air-passenger reduction by great-circle distance for cumulative lever bundles (passenger-weighted), built up from electrification to electrification+autonomy, to AVcore (the headline, bold), to AVcore+aviation carbon price, to AVcore+carbon price+speed; the response decays with distance. Car speed is shown only as a top-of-stack increment, since it is meaningful only once automation is present. (b) Most-affected routes: personal air passengers in the base (light) with the post-AVcore remainder (dark) overlaid, so the gap is the switching; each bar is annotated with its percentage reduction. (c) Most-affected airports, by total personal air passengers shifted to car summed over the routes touching each. Both-hub connection-trunk routes are excluded throughout.

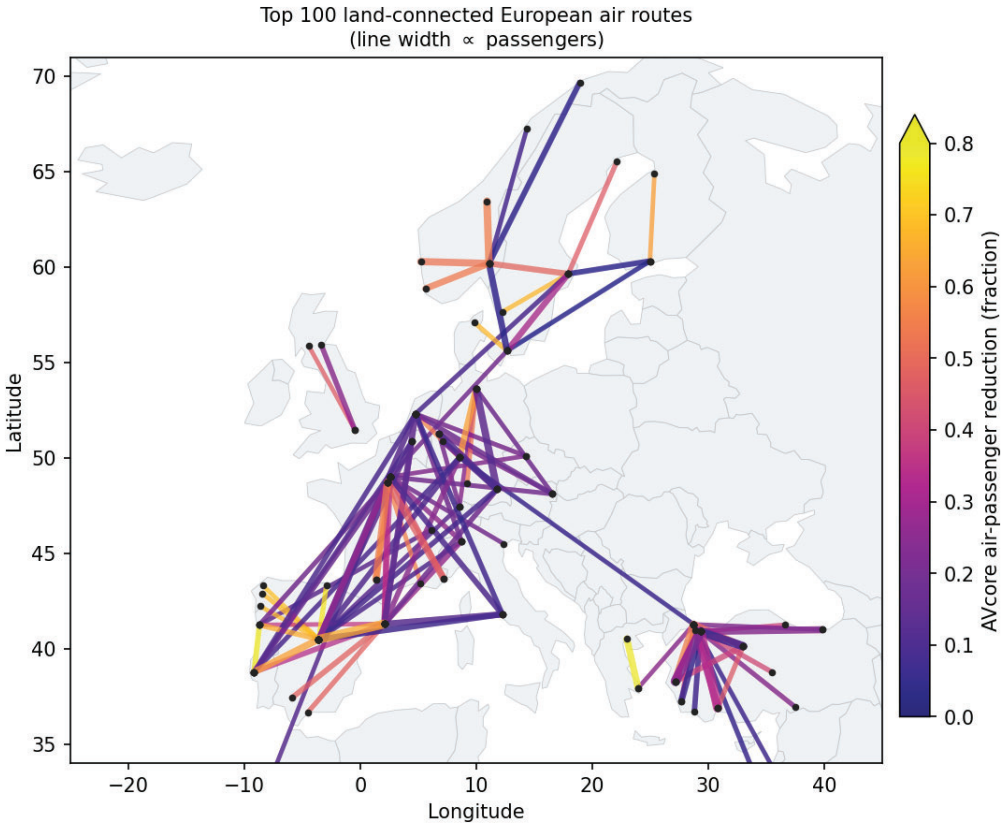


Figure 2: The top 100 land-connected European air routes by passenger volume. Line width is proportional to passengers and colour is the AVcore air-passenger reduction (scale capped at 0.8, just beyond the largest route effect): substitution concentrates on short, dense corridors.

5.2 The passenger–emissions asymmetry

Large passenger shifts translate into small emissions savings, because within intra-European aviation short-haul carries a disproportionate share of passengers but a small share of emissions (Table 1). The land-connected subset AV can reach is 57 % of passengers but only 49 % of CO_2e (80 of 164 Mt); the remaining 43 % of passengers are on island and cross-water corridors – the Balearics, Canaries, Greek islands and the Channel and Irish-Sea crossings – that no road journey can substitute. The AVcore shift removes about a fifth of the land-connected base emissions (18.8 %, 15.1 Mt): mode shift is a real but bounded lever, reaching the many short flights, not the longer ones that dominate emissions. These figures already net out the bulk of connecting traffic, so the addressable share is not inflated by trips that cannot switch (Sections 4 and 5.4). Because the substitute is the same clean-grid electric fleet the social-cost layer assumes, a switched flight's warming is avoided almost in full, so this is effectively the *gross* aviation CO_2e removed; charging the replacing car at today's grid instead would trim the saving to about 13 Mt (a sixth).

This bound is robust to the aviation emissions factor. The addressable share is a *ratio*, so any uniform rescaling of intensity – including the non-CO_2 warming multiplier – leaves the gross avoided share unchanged; only the distance *profile* of intensity moves it (Table 4). Even an adverse profile – a non-CO_2 multiplier rising with distance (1.5 to 3.0, mean held at 2.0), as contrail and NO_x forcing concentrates in long-haul cruise – pushes CO_2e onto the unsubstitutable long haul and only lowers the share, to 17.1 %. Across every specification the shift addresses about a fifth (16 % to 19 %) of reachable land-connected CO_2e; if anything, a richer treatment of non-CO_2 forcing strengthens the asymmetry.

Table 4: Addressable CO_2e share under alternative aviation emissions factors (% of *land-connected* personal aviation CO_2e removed by the AVcore shift). The share is invariant to a uniform rescaling; only the distance profile of intensity moves it.

Emissions-factor assumption	Addressable share (%)
Distance-banded, non-CO_2 $\times 2$ (base)	18.8
Flat 0.15 kg/pkm, non-CO_2 $\times 2$	16.3
Rising non-CO_2 multiplier with distance	17.1

5.3 Social cost of the shift

Under AVcore, about 93 million personal trips switch from air or rail to car, averaging 587 km; 84 million come from aviation and 9 million (10 % of switchers) from rail, reflecting rail's

small personal role.[1] Table 5 reports the net external effect (equation (8)) under two labels: *Main*, our central AV+EV world in which the substitute cars are clean and automated, and *ICE-today*, the same switching re-valued at 2019 ground technology – an accounting decomposition, not a scenario (the switching is induced by autonomy, so a genuine 2019 world would see none of it), which isolates how much of the benefit comes from the incoming fleet being clean *and* safe rather than from avoiding flights.

At the aggregate level the shift removes about a fifth of the reachable aviation's own external cost – from about 10.8 to 8.7 bn € a year, some three-quarters of it avoided climate and upstream-fuel damage and concentrated in the distance-scaling categories (Figure 3a). Per switching trip the balance is finer, because the substitute car brings its own external costs.

In the *Main* case the average trip's external cost falls from 23.94 € flown to 18.18 € driven – a *saving* of 5.76 € per trip (0.98 ct/pkm). [2] At 2019 technology the same reallocation is instead a net *cost* of 12.60 € per trip (external cost *rising* from 29.15 € flown to 41.75 € driven, because a 2019 car is dirty and unsafe). The two valuations of the same switched trips differ by about 18 € per trip, split between the accident term – the car accident externality is scaled by 0.10 (Section 2.4) as automation removes the roughly nine-tenths of crashes attributable to human error, so once avoided air-side accidents are netted against the small residual road-side cost the net all but vanishes – and the climate term, since the electric car has no tailpipe carbon whereas a 2019 car's climate cost offsets much of the avoided flight; avoided air pollution and upstream fuel are smaller.

By category (*Main*, €/trip), the saving is a large avoided-climate benefit (+13.2) and well-to-tank (+4.1), offset by habitat/land-take (−6.2), noise (−2.5) and congestion (−2.4) from the extra car travel, with accidents and air pollution near zero once the car is clean and automated.[3] The net is a difference of large opposing terms, which is why it is small

[1] The switchers skew solo: about 55 % travel alone (against a 45 % population share), because automation cuts the driver's time penalty – the largest slice of a lone traveller's car cost, which they cannot share. This composition drives the per-trip balance below: aviation's cost is per passenger but the car's noise and land-take are per vehicle, so with occupancy 1.6/N the switch is a net *cost* of about 2.50 € for a solo switcher and a saving of about 18 € for a party of four. Weighting each party by its own occupancy gives a blended 4.58 €, below the 5.76 € headline, which applies the mix-average occupancy uniformly; the gap is the solo–switching correlation the headline averages away, the solo majority carrying the highest per-passenger car cost.

[2] The estimation uncertainty in the structural parameters affects the *volume* of switching far more than this per-trip balance, which is a difference of external-cost rates independent of the behavioural parameters; the substantive uncertainty in the *sign* is the aviation-decarbonisation dial and carbon value, not the estimated parameters.

[3] Noise is a net *cost* because the handbook (van Essen et al., 2019a) books the two modes' noise differently: aviation noise is a per-flight landing/take-off charge, road noise a per-kilometre cost along the whole corridor. Over a ∼600 km trip the accumulated road noise exceeds the flight's, and electrification gives no relief at motorway speed, where tyre/road noise dominates.

and sensitive (Figure 3).

Two simplifications leave the central figure, if anything, conservative. First, we omit airport access entirely: flying really does incur road trips to and from airports, but CE Delft has no dedicated measure for them, and – since we value the substitute car at motorway rates over the whole drive, uncharged for its own urban ends – crediting the flight with all-roads access at both ends would be asymmetric; omitting it understates the avoided cost. Second, the habitat/land-take and noise terms charge the handbook's *average* per-passenger-kilometre cost, but most motorway land-take is sunk and the *marginal* cost of one more inter-city trip on an existing motorway is close to zero, so the average overstates the road-side drag. Both point the same way, so 5.76 € is our best – and likely conservative – central figure.

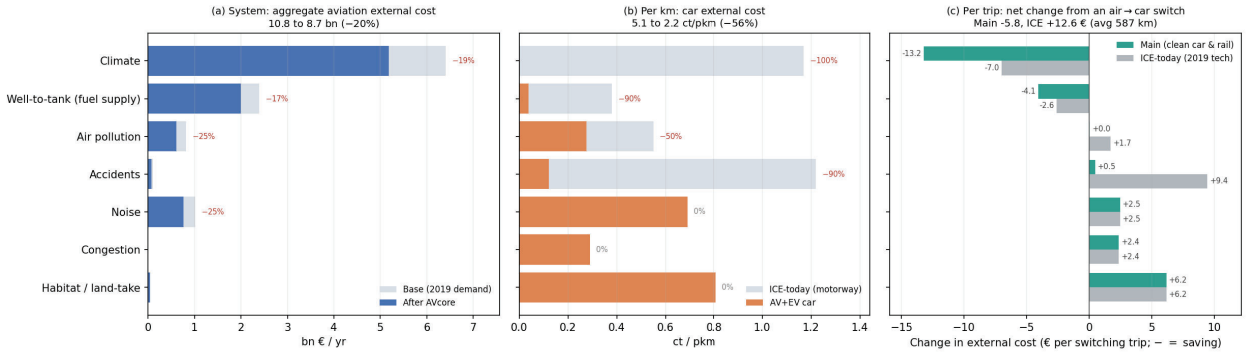


Figure 3: The social cost of the shift at the three valuation levels of Section 1, by CE Delft cost category (ordered combustion-linked first, then always-on road costs). **(a) System:** aggregate external cost of the land-connected personal aviation the car can reach, base (2019 demand) with the post-AVcore remainder overlaid, each bar annotated with its % reduction; the shift removes about a fifth (10.8→8.7 bn €/yr). **(b) Per km:** the substitute car's own external cost, the ICE-today car versus the AV+EV car – a clean fleet more than halves it (5.1 ct/pkm to 2.2 ct/pkm), zeroing climate and all but eliminating accidents, but leaving noise, congestion and land-take untouched. **(c) Per trip:** the per-category change in external cost from an air/rail→car switch, *Main* (clean) versus *ICE-today* (negative = a saving, matching panels a–b); the small net saving under *Main* (−5.8 €) is the residual of a large avoided-climate benefit against the extra road costs, and becomes a net cost at 2019 technology (12.6 €), so the case rests on the incoming fleet being clean *and* safe. Airport access is excluded throughout.

Because the benefit relies on avoided aviation climate cost, how fast aviation decarbonises sets the sign (lower block of Table 5). Holding the clean car fixed at 18.18 € and dialing only aviation: at a 2019 emissions level the flight is worth avoiding by 10.68 € per trip; under our modest base, 5.76 €; under aggressive SAF adoption the flown cost falls below the car, so the shift becomes a *cost* (−1.35 €). The social-cost case for AV-driven mode shift is strongest

when aviation is slowest to abate.

Both the valued climate damage and the carbon-price lever are set at 100 €/t CO_2 – conservative for a 2050 horizon, where most social-cost-of-carbon trajectories are materially higher. Since the avoided-climate benefit scales roughly with the carbon value, a 2050-appropriate price would widen the per-trip saving and make its sign more robustly positive, though the same high price would also hasten the aviation abatement that works the other way.

Table 5: Net external effect of the AVcore shift (+ = social saving), per switching trip, per passenger-kilometre and in aggregate. "Flown" is the trip's external cost before the switch (as air/rail; rail legs valued at the scenario's ground-fleet technology), "driven" after (as car); net = flown − driven. *ICE-today* re-values the same switching at 2019 ground technology (a clean, automated car replaced by a 2019 car) as an accounting decomposition. The three *Main* rows hold the incoming car clean and automated and dial only aviation decarbonisation by the scenario horizon (2019 level → modest base → aggressive sustainable fuel).

Case	Flown €	Driven €	Net € / trip	ct / pkm	bn €/yr
ICE-today (both 2019)	29.15	41.75	−12.60	−2.15	−1.17
Main, aviation 2019 level	28.86	18.18	+10.68	+1.82	+0.99
Main, aviation modest (base)	23.94	18.18	+5.76	+0.98	+0.53
Main, aviation aggressive SAF	16.83	18.18	−1.35	−0.23	−0.12

5.4 Robustness

Table 6 reports the fit and headline across specifications, with detail in Appendix B. The cliff elasticity is stable throughout and the AVcore shift moves only modestly around its 24.6 % base under every statistical choice. A single pooled elasticity rather than the two-regime split raises it, as the near-deterministic long-haul routes pull the pooled elasticity up and over-state substitution on drivable corridors; dropping the country and international air constants raises it only modestly, confirming they act as level shifts (row D vs A); equal route weighting lifts it (row F), so our passenger weighting is the conservative choice; and tolls in the base lower it (row E). The connection-traffic treatment (Section 4) removes exactly the non-substitutable connecting passengers that would otherwise inflate the shift. The one first-order lever is behavioural, not statistical: the driver-time penalty γ *is* the autonomy mechanism, so the shift scales with it from 18 % to 32 % across γ's plausible range (rows G–H), whereas the transferred party-size mix (rows I–J, absorbed by the re-estimated VTT) and a single Europe-wide VTT leave it within a few points. The passenger–emissions asymmetry and the social-cost conclusions hold throughout.

Table 6: Robustness of the model fit and the AVcore headline to the elasticity specification, the country/international air ASCs, road tolls, route weighting and the transferred party-size assumptions. Rows are labelled A–J and referenced by letter in the text. Statistical rows (A–F) are re-fit and scored uniformly over genuine land-connected routes, passenger-weighted (row A is the production spec of Table 2, scored on the reported route set); the headline is the AVcore air-passenger reduction and CO_2 saving on the reported route set. σ_s/σ_l are the drivable/long-haul elasticities (the single-elasticity row has one σ), transitioning continuously across the profiled regime midpoint (held at 15 h); χ is the value of travel time in €/h. Rows G–J vary the *transferred* party-size assumptions (re-estimating the identified parameters, so χ moves; σ_l and MAE omitted): the driver-time uplift γ over its plausible range (G–H, the one first-order behavioural lever) and the party-size mix from solo- to group-heavy (I–J).

Specification	σ_s	σ_l	χ	MAE	AVcore cut / CO_2
A. Production (country FE + intl)	3.29	5.44	16.8	0.093	24.6% / 15.1 Mt
Single elasticity (country FE + intl)	4.16	–	16.3	0.094	26.6% / 16.5 Mt
B. Country FE only	3.66	5.89	17.5	0.096	27.7% / 17.1 Mt
C. International only	3.14	5.26	16.3	0.107	24.2% / 14.8 Mt
D. No ASCs (structural core)	3.30	5.53	19.3	0.111	26.2% / 16.2 Mt
E. Production + tolls in base	3.31	5.71	13.7	0.094	23.2% / 14.2 Mt
F. Prod. + equal route weighting	2.94	5.11	12.3	0.111	28.6% / 18.5 Mt
G. Low driver-time penalty ($\gamma = 1.35$)	3.21	–	20.4	–	18.2% / 10.9 Mt
H. High driver-time penalty ($\gamma = 2.10$)	3.33	–	11.7	–	32.0% / 20.4 Mt
I. More solo (.60/.25/.08/.07)	3.14	–	12.1	–	27.2% / 17.2 Mt
J. More groups (.30/.30/.15/.25)	3.27	–	18.1	–	22.1% / 13.2 Mt

6 Discussion and limitations

The scope is deliberately narrow – personal, non-connecting, land-connected intra-European travel: business travel and onward-connecting itineraries are excluded because the model is a leisure, point-to-point construct, and the land-connected requirement further sets aside the island and cross-water corridors (Section 5) that no road trip can substitute. Our headline percentages are measured against this land-connected subset (the passenger and CO_2e shares are given in Sections 3 and 5). Within that scope, four caveats bound the interpretation.

First, the model is a long-run comparative static: it characterises the equilibrium re-allocation once a mature autonomous-electric fleet is in place, and says nothing about the transition *path* – the rate of fleet turnover or the order in which corridors tip.

Second, it is pure substitution accounting and omits *induced demand*: cheaper, more comfortable car travel may generate entirely new car trips whose emissions and externalities

we do not count. On the aviation side a fall in demand may *reinforce* the shift rather than rebound against it – thinner routes lose frequency and, if carriers exit, fares worsen, pushing further travellers to land transport – but we model neither supply response.

Third, the ground modal split we validate against is 2010 (ETISplus), with no newer public origin–destination dataset available; our vintage correction anchors air demand to 2019 but cannot refresh the 2010 ground modal structure, which is the source of a handful of low-volume corridors – chiefly in eastern Turkey – with implausibly high observed car shares (Appendix C). These carry under 1 % of validation passengers and do not affect any weighted result. As external context, Eurostat's aggregate inland modal split has been broadly stable since 2010 – cars have held about four-fifths of inland passenger-kilometres and rail under a tenth, with no large car–rail reallocation (Eurostat, 2023); the visible change over the period is the growth of intra-European aviation, which our vintage correction already anchors to 2019. The 2010 ground structure is therefore unlikely to misstate the aggregate car–rail split, even if it cannot capture route-level change.

Fourth, the low rail-to-car leakage (10 % of switchers) reflects the sparse leisure rail use of the 2010 network we observe; a denser future high-speed network would draw more of the AV-induced switching out of clean trains, eroding the net saving, so our leakage is a lower bound conditional on 2010 rail supply. Two modelling features reinforce this reading: all pairwise substitution runs through the CES elasticity (there is no separate rail–car cross-elasticity), and rail's alternative-specific constants are weakly identified because rail is only about 2 % of the personal market. Neither materially affects the headline, which is dominated by the far larger air–car margin, but both mean the rail leg should be read as an order of magnitude rather than a precise figure.

The policy reading is therefore twofold. The shift is a genuine, no-cost decarbonisation lever: a mature autonomous electric fleet draws a substantial minority of personal air passengers off short-haul flights and removes about a fifth of the CO_2e it can reach – a material dividend the aviation-decarbonisation ledger currently counts as zero, and one that arrives without any carbon price or fuel mandate. But it is no substitute for supply-side action – the long-haul flights that dominate CO_2e lie beyond its reach – and its *social* value does not follow automatically from the behavioural response: whether the switching is a net gain at all rests on the incoming fleet delivering both of its improvements at once. Electrification is what makes the avoided flight worth taking, and automation is what stops the extra driving from importing a large accident cost.

7 Conclusion

Estimating a three-mode disutility model on European personal travel, we find that mature autonomous electric vehicles could shift about a quarter (24.6 %, and 18 % to 32 % across the plausible range of the driver-time penalty) of land-connected personal air passengers to cars. The consequences separate into three. At the *system* level the shift reaches about a fifth (19 %) of the reachable aviation CO_2e – and cuts its external cost by about the same share – a material, no-cost dividend that is nonetheless bounded, because emissions live in the longer flights cars cannot replace. *Per kilometre* the substitute is far cleaner: electrification and automation more than halve driving's own external cost. *Per switching trip* the two net to a modest social saving – the external cost falls from about 24 € flown to 18 € driven, roughly 6 € (about 1 ct/pkm over the average 587 km switch) – the small residual of a large avoided-aviation climate benefit against extra road noise, land-take and congestion. That residual is a net cost for the solo travellers who make up most switchers, hinges on the car fleet being clean and safe, and turns negative overall if aviation decarbonises quickly.

References

Simon P. Anderson, André de Palma, and Jacques-François Thisse. *Discrete Choice Theory of Product Differentiation*. MIT Press, Cambridge, MA, 1992.

Frédéric Dobruszkes. High-speed rail and air transport competition in western europe: A supply-oriented perspective. *Journal of Transport Geography*, 19(4):870–879, 2011. doi: 10.1016/j.jtrangeo.2010.09.004.

EASA and EEA and EUROCONTROL. European aviation environmental report 2022. Technical report, European Union Aviation Safety Agency, Cologne, 2022.

Jonathan Eaton and Samuel Kortum. Technology, geography, and trade. *Econometrica*, 70 (5):1741–1779, 2002. doi: 10.1111/1468-0262.00352.

ETISplus Consortium. Etisplus: European transport policy information system – database and reference scenario (base year 2010). Technical report, European Commission, Seventh Framework Programme, 2013.

European Union. Directive 2008/101/ec amending directive 2003/87/ec so as to include aviation activities in the scheme for greenhouse gas emission allowance trading within the community, 2009. Official Journal of the European Union, L 8, 13 January 2009.

European Union. Regulation (eu) 2023/2405 of the european parliament and of the council on ensuring a level playing field for sustainable air transport (refueleu aviation), 2023. Official Journal of the European Union, L series, 31 October 2023.

Eurostat. Modal split of inland passenger transport (dataset tran_hv_psmod). Statistical Office of the European Union, Luxembourg, 2023. Passenger-kilometres by car, rail and bus; accessed 2024.

Krishna Murthy Gurumurthy and Kara M. Kockelman. Modeling americans' autonomous vehicle preferences: A focus on dynamic ride-sharing, privacy and long-distance mode choices. *Technological Forecasting and Social Change*, 150:119792, 2020. doi: 10.1016/j.techfore.2019.119792.

International Energy Agency. Net zero roadmap: A global pathway to keep the 1.5 °c goal in reach – 2023 update. Technical report, International Energy Agency, Paris, 2023. URL `https://www.iea.org/reports/net-zero-roadmap-a-global-pathway-to-keep-the-15-0c-goal-in-reach`.

Jeffrey J. LaMondia, Daniel J. Fagnant, Hongyang Qu, Jackson Barrett, and Kara Kockelman. Shifts in long-distance travel mode due to automated vehicles: Statewide mode-shift simulation experiment and travel survey analysis. *Transportation Research Record*, 2566 (1):1–11, 2016. doi: 10.3141/2566-01.

D. S. Lee, D. W. Fahey, A. Skowron, M. R. Allen, U. Burkhardt, Q. Chen, S. J. Doherty, S. Freeman, P. M. Forster, J. Fuglestvedt, A. Gettelman, R. R. De León, L. L. Lim, M. T. Lund, R. J. Millar, B. Owen, J. E. Penner, G. Pitari, M. J. Prather, R. Sausen, and L. J. Wilcox. The contribution of global aviation to anthropogenic climate forcing for 2000 to 2018. *Atmospheric Environment*, 244:117834, 2021. doi: 10.1016/j.atmosenv.2020.117834.

Dennis Luxen and Christian Vetter. Real-time routing with openstreetmap data. In *Proceedings of the 19th ACM SIGSPATIAL International Conference on Advances in Geographic Information Systems (GIS '11)*, pages 513–516, 2011. doi: 10.1145/2093973.2094062.

Maren Outwater, Mark Bradley, Nazneen Ferdous, Stephen Trevino, and Hsi-Hwa Lin. Foundational knowledge to support a long-distance passenger travel demand modeling framework. Technical Report Project C04, Strategic Highway Research Program 2 (SHRP 2), Transportation Research Board, Washington, DC, 2015.

Kenneth A. Perrine, Kara M. Kockelman, and Yantao Huang. Anticipating long-distance

travel shifts due to self-driving vehicles. *Journal of Transport Geography*, 82:102547, 2020. doi: 10.1016/j.jtrangeo.2019.102547.

Patrick A. Singleton. Discussing the "positive utilities" of autonomous vehicles: will travellers really use their time productively? *Transport Reviews*, 39(1):50–65, 2019. doi: 10.1080/01441647.2018.1470584.

Jork Stapel, Freddy A. Mullakkal-Babu, and Riender Happee. Automated driving reduces perceived workload, but monitoring causes higher cognitive load than manual driving. *Transportation Research Part F: Traffic Psychology and Behaviour*, 60:590–605, 2019. doi: 10.1016/j.trf.2018.11.006.

Roger Teoh, Zebediah Engberg, Marc Shapiro, Lynnette Dray, and Marc E. J. Stettler. The high-resolution global aviation emissions inventory based on ADS-B (GAIA) for 2019–2021. *Atmospheric Chemistry and Physics*, 24:725–744, 2024. doi: 10.5194/acp-24-725-2024.

Christer Thrane. Examining tourists' long-distance transportation mode choices using a multinomial logit regression model. *Tourism Management Perspectives*, 15:115–121, 2015. doi: 10.1016/j.tmp.2015.05.004.

Huib van Essen, Lisanne van Wijngaarden, Arno Schroten, Daniel Sutter, Cuno Bieler, Silvia Maffii, Marco Brambilla, Davide Fiorello, Francesca Fermi, Riccardo Parolin, and Kareen El Beyrouty. Handbook on the external costs of transport, version 2019. Technical report, European Commission, Directorate-General for Mobility and Transport (CE Delft), Brussels, 2019a.

Huib van Essen, Lisanne van Wijngaarden, Arno Schroten, et al. Sustainable transport infrastructure charging and internalisation of transport externalities: Main findings. Technical report, European Commission, Directorate-General for Mobility and Transport (CE Delft), Brussels, 2019b.

Zia Wadud, Don MacKenzie, and Paul Leiby. Help or hindrance? the travel, energy and carbon impacts of highly automated vehicles. *Transportation Research Part A: Policy and Practice*, 86:1–18, 2016. doi: 10.1016/j.tra.2015.12.001.

Anthony Wiskich. Take me home, country roads: Choosing autonomous EVs over personal aviation. *Australian Journal of Agricultural and Resource Economics*, 0:1–13, 2026. doi: 10.1111/1467-8489.70158.

A Parameters and calibrated inputs

The five structural parameters and the reduced-form air constants are estimated by unpenalised maximum likelihood on the European personal modal splits; the point estimates and bootstrap standard errors are in Table 2.

The remaining inputs are calibrated to external data rather than estimated; Table 7 collects them all – engineering constants, the fare curve, emission factors, external unit costs and the future-world adjustment factors – with their values and sources, and the salient ones are discussed here. *Air detour*: flown distance is the great-circle distance times an empirical detour factor from the GAIA global flight inventory (Teoh et al., 2024). Its public outputs give the flown/great-circle ratio for a large set of 2019 origin–destination pairs; we use a route's own ratio where available and otherwise a curve detour $= 1 + A\, d^{B-1}$ (with $A = 1.05$, $B = 0.58$, d in km) fitted to ∼19 000 pairs, in which the absolute extra distance grows sub-linearly, so the ratio falls from ∼1.13 at 150 km to ∼1.03 at 4000 km. *Fares*: a single Europe-wide yield curve $\Phi + \Upsilon \max(0, d-500)$ with a sub-500 km plateau (Section 2); regional and route-level fare multipliers were tested and did not improve out-of-sample fit, so the flat curve is retained. *Engineering constants* (cruise speed, fixed airport/access times, rail access time and frequency-to-wait mapping) and the *external-cost layer* (CE Delft handbook) are taken directly from the sources. *Tolls* enter only the sensitivity re-estimation (row E of Table 6); the effective whole-drive-averaged rates, and the large fixed crossings amortised over the drive, are listed in Table 7.

Table 7: Calibrated (non-estimated) inputs and their sources. Monetary values in euros (source values in AUD converted at 1.65 AUD/€). The value of travel time χ and the other *estimated* behavioural parameters are in Table 2; external unit costs are in cents per passenger-kilometre (2016 prices), with the category order given at the head of that block.

Input	Value	Source
Air: engineering and fare		
Cruise speed S	850 km/h	Engineering; Wiskich (2026)
Fixed non-cruise time Γ	4.39 h	Wiskich (2026)
Airport financial access Ψ (per airport, per party)	25.8 €	Wiskich (2026)
Fare intercept Φ	62.5 €	EU short-haul yield calibration
Fare slope Υ (beyond 500 km)	0.075 €/km	EU yield calibration
Average-fare uplift Ω	1.00	EU yields already average

continued on next page

Table 7, continued

Input	Value	Source
Fare kink distance	500 km	Wiskich (2026)
Detour curve $1 + A\,d^{B-1}$	$A = 1.05,\ B = 0.58$	Fit to GAIA (Teoh et al., 2024)
Car		
Baseline speed	90 km/h	Network-average assumption
Variable cost π	0.16 €/km	European fuel + running cost
Road tolls (sensitivity only; €/km, whole-drive avg.)	FR .055, IT .050, PT .060, GR/HR .045, ES .035, NO .030, TR .025, PL .015, IE .010 (free/vignette elsewhere); fixed crossings Izmir–Istanbul ∼45, Øresund ∼50 € amortised	National toll operators, 2024 tariffs
Transferred behavioural inputs (not estimated)		
Driver VTT uplift γ	1.69	Wiskich (2026)
Party-size mix ($N = 1, 2, 3, 4$)	.45 / .30 / .10 / .15	Outwater et al. (2015)
Rail		
In-vehicle speed (fallback)	120 km/h	ETISplus (ETISplus Consortium, 2013)
Route detour factor	1.20	ETISplus
Access time a_r / distance (each end)	1.0 h / 5 km	City-centre-station assumption
Service window; wait cap	16 h; 3 h	ETISplus frequencies
In-vehicle time, frequency, fare	observed, per route	ETISplus (ETISplus Consortium, 2013)
Emissions factors		
Aviation CO_2 intensity, banded (kg/pkm), 0–500 / 500–1100 / 1100–2200 / 2200–4000 / 4000+ km	0.185 / 0.125 / 0.105 / 0.098 / 0.108	ICAO/myclimate economy-class curves
Non-CO_2 warming multiplier	2.0	Lee et al. (2021)
EV consumption; grid intensity	0.18 kWh/km; 0.30 kg/kWh	European fleet/grid average
EV grid decarbonisation (AV world)	$\times$ 0.10 on grid	Clean-grid future; matches car WTT cost adj.
Rail traction intensity	0.035 kg/pkm	European electrified-rail average

continued on next page

Table 7, continued

Input	Value	Source
Car occupancy (emissions)	1.5	EU average; cf. handbook occupancy 1.6
External unit costs (ct/pkm, 2016 prices; category order: accidents / air poll. / climate / noise / congestion / WTT / habitat)		
Car, motorway (categories; total)	1.22 / 0.55 / 1.17 / 0.69 / 0.29 / 0.38 / 0.81; **5.11**	CE Delft, motorway Table 122 (van Essen et al., 2019a)
Rail (categories; total)	0.50 / 0.12 / 0.05 / 0.90 / 0.00 / 0.70 / 0.60; **2.87**	CE Delft (van Essen et al., 2019a)
Aviation total by band (<1500 / 1500–4000 / 4000+ km)	4.3 / 2.8 / 3.2	CE Delft synthesis (van Essen et al., 2019a)
Aviation LTO vs cruise split; reference distance	LTO (fixed per flight): noise, air poll., accidents, habitat; cruise (per km): climate, WTT; $D_{\text{ref}} = 1500\,\text{km}$	Authors' split of CE Delft categories
Carbon value	100 €/t CO_2	CE Delft central
Scenario levers, car side (Section 2.3)		
EV running-cost drop (**ev**)	0.09 €/km (π: 0.16→0.07)	Wiskich (2026)
Overnight (**on**): sleep; VTT factor; cost add; take-up	8 h; 0.5; +0.12 €/km; 50 %	Wiskich (2026)
Speed boost (**spd**)	+10 km/h on 90 km/h	Wiskich (2026)
Future-world external-cost adjustment factors (multiplicative on 2016 rates)		
Car AV+EV: accidents / climate / air poll. / WTT (others 1.0)	0.10 / 0.05 / 0.50 / 0.20	Author assumptions (sensitivity layer)
Rail future: climate / WTT / air poll. (others 1.0)	0.40 / 0.30 / 0.50	Author assumptions
Aviation base "modest": climate / air poll. / WTT (others 1.0)	0.80	Flexed in Table 5

B Robustness detail

This appendix expands each row of Table 6 and the party-size sensitivity summarised in Section 5.4.

Country and international air constants. The reduced-form country and international air constants (row A) tighten the fit – cutting the vertical dispersion of routes around the cost index by about a sixth relative to a purely structural specification (row D) – yet barely move the headline: dropping them *raises* the AVcore shift only modestly (row D vs A), as the constants pin some high-air corridors to their observed level. The country effect is national rather than a route-geometry artefact: a road-detour barrier proxy (standing in for sea crossings) carries no residual signal once the constants are present, and road tolls neither improve the fit nor substitute for them. Equal route weighting (row F) lifts the shift, amplifying the many short, car-competitive corridors, so the air-passenger weighting of the headline is the more conservative choice.

Transferred party-size assumptions. Because the party-size structure is transferred, we re-estimate the identified parameters under alternatives and recompute the headline (rows G–J). Varying the party mix from solo- to group-heavy (rows I–J) moves the shift only within a few points of the headline, because the re-estimated value of travel time absorbs the change. The driver VTT uplift γ is different – it *is* the autonomy lever, the removal of the driver-time penalty – so the shift scales with it across γ's plausible range (rows G–H). This is not fragility but the central behavioural assumption: how much substitution autonomy induces depends first on how strongly travellers dislike driving, and only second on trip composition. Our $\gamma = 1.69$ is the estimate of Wiskich (2026).[4]

Connection-contaminated routes. The three-tier connection treatment – the 12 both-hub *trunk* routes excluded and the 59 single-hub *feeders* pivoted onto their observed base by the nuisance air constant – is set out in Section 4. Without it – counting the trunks and giving feeders the full modal-cliff response – both the AVcore shift and the addressable CO_2e would be inflated by exactly the non-substitutable connecting traffic. (A separate handful of long, low-volume eastern-Turkish corridors are a 2010-vintage artefact, handled by the vintage-consistent target rather than by exclusion; Appendix C.) The study is thus best read as the personal, non-connecting subset of intra-European aviation.

Road tolls. The headline base carries no road tolls. Because tolls already applied in the observed base year, a with-tolls world requires *re-estimating* with tolls in the base (row E)

[4]As external context, the price paid for *partial* automation gives a rough market read on the value of relief from driving: Tesla's Full Self-Driving subscription runs about 90 € a month, whereas at our estimates the driver-time relief is worth $(\gamma - 1)\chi \approx 11.6$ €/h – several hundred euros a month for a typical motorist. The comparison is loose, since today's systems still require supervision (Stapel et al., 2019) and our leisure χ likely understates these mostly-commuting kilometres.

– not bolting them onto the toll-free forward model, which would break the base fit. Doing so moves the parameters only modestly (row E) and damps the AVcore shift by about a percentage point, leaving the addressable share at 17.7 % of the land-connected base and the passenger–emissions asymmetry and social-cost conclusions intact. The toll schedule is listed in Appendix A.

A single value of travel time. A single Europe-wide χ cannot resolve variation across corridors or income groups, but the aggregate is insensitive to it: an income-scaled VTT (χ proportional to regional GDP per capita) returns an income elasticity indistinguishable from zero ($\eta = 0.00$, SE 0.10) with no out-of-sample gain, and a GDP-weighted VTT leaves the shift within a percentage point. What the representative χ cannot describe is the *composition* of who switches, which is why the headline is best read as an aggregate rather than a statement about any corridor or traveller.

C Validation diagnostics

Vintage correction. The estimation and validation target splices 2019 air demand onto the 2010 ground network. For each route we form an air-growth proxy

$$g = \frac{\text{2019 Eurostat air pax}}{\text{2010 ETISplus air trips}},$$

and confirm that the model's air-share error against the raw 2010 benchmark rises with g – the residual is post-2010 demand growth, not model misfit. We therefore rebuild air volume from the 2019 count, keeping the 2010 car and rail volumes, converting Eurostat passengers to ETISplus air-trip units by a single global constant k (their cross-route median). Because a single k would wrongly *shrink* the few heavy trunk corridors whose 2010 base already far exceeds the median (Barcelona–Madrid, at ∼14× the median, would collapse from a real ∼23 % air share toward 2 %), and because aviation did not contract over 2010–2019, the correction is applied one-sidedly,

$$\text{air volume} = \max\big(\text{own 2010 ETISplus air},\ k\text{-scaled 2019 air}\big),$$

so it only ever *raises* stale 2010 benchmarks (chiefly the post-2010 Turkish and eastern-European boom corridors) and never lowers them. Modal shares are then recomputed from the spliced volumes.

Figure 4 plots predicted against observed personal mode shares (point area ∝ passengers,

colour = great-circle distance). The distance colouring explains the main features: the near-zero *car* and near-unity *air* shares are the long routes (Amsterdam–Barcelona, Paris–Rome) on which almost everyone flies – correct modal-cliff behaviour, not water crossings (ferries are excluded by the land-connected filter) – and the model places them in the corners. Two of the three residual patterns are issues already handled: the long, low-volume eastern-Turkish corridors with implausibly high *observed* car (2010-vintage artefacts the model rightly declines to reproduce), and the short hub feeders with connection-inflated observed air (both treated in Section 4). The only genuinely residual miss is a small air over-prediction (about 0.05) between 400 km to 800 km on strong-rail leisure corridors (Spanish AVE, Greek and Iberian coastal pairs), the limit of the single-index form – and none of the three materially affects the passenger-weighted results.

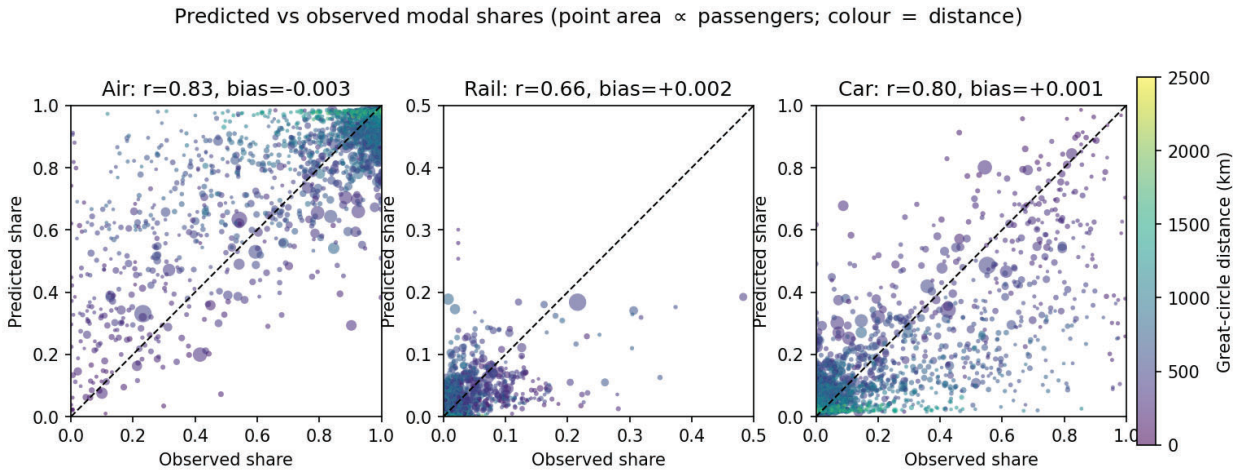


Figure 4: Predicted versus observed personal modal shares (point area $\propto$ passengers; colour = distance); dashed line is 45°.

Figure 5 shows the air-share gradient two ways. Against great-circle distance (panel (a)) the observed shares rise in a modal "cliff" the model tracks; the faded curves are the fit at fixed party sizes $N = 1 \ldots 4$ (larger parties share the car's cost, so fly less) and the reported line their party-mix average. Against the model's own air/ground generalised-cost ratio (panel (b)) – which folds in VTT-weighted time, fares, detour, tolls, party-size cost-sharing and graded rail – the same shares collapse onto the CES curve (two-regime elasticity taken per route from drive time), and the fit improves on distance alone; party size here enters through the ratio itself, so a per-N curve would coincide.

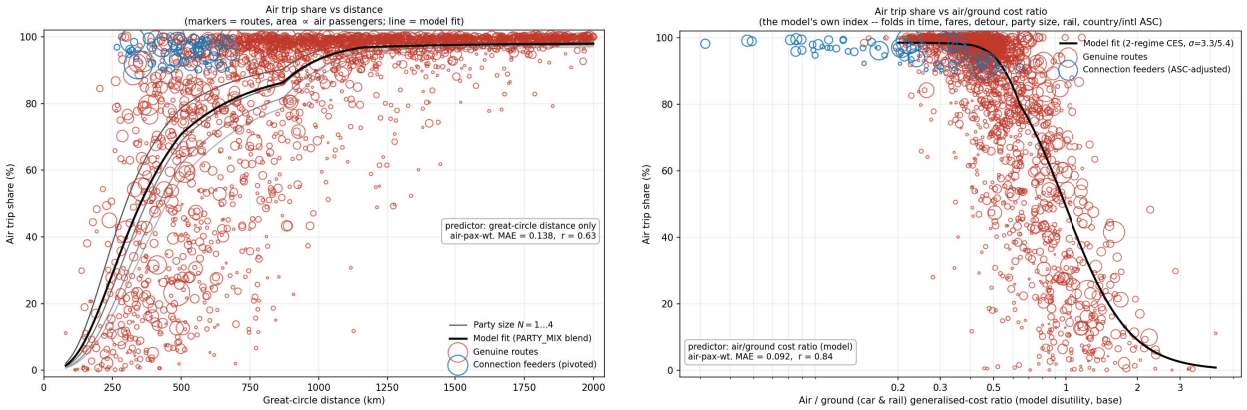


Figure 5: Air-trip share two ways (markers = routes, area $\propto$ air passengers; among the large labelled markers genuine routes are red and single-hub connection feeders blue, and both-hub connection-trunk routes are excluded). **(a, left)** versus great-circle distance: the black line is the model fit for a representative land-connected route (party-mix blend), the faded grey lines the same fit at fixed party sizes $N = 1 \ldots 4$; the shares rise in a modal "cliff" the model tracks. **(b, right)** versus the model's air/ground generalised-cost ratio, the index the three-mode model actually uses: air share is a tight declining logistic in this ratio, whereas against raw distance it is bimodal at a given range.

D Most-affected routes and airports

Figure 6 lists the 40 busiest land-connected corridors (by personal air passengers), ordered by volume, with the base air traffic (light) and the post-AVcore remainder (dark) overlaid so the gap is the shift, and each bar labelled with its percentage reduction. Ranking by volume rather than by absolute shift shows how the reduction lands on the routes that actually carry the traffic, and makes the heterogeneity in the modal-cliff position explicit: the percentage reduction ranges from single digits on the connection feeders retained with the nuisance constant (e.g. Hamburg–Munich, Copenhagen–Oslo) to 70 % or more on genuine short-haul leisure corridors.

Figure 7 takes the airport view and restores the geographic context the route figure omits. For each of the 40 busiest airports by *total* personal intra-European air, it draws three nested tiers: all personal intra-European air at the airport (every route, including the island, cross-water and long-haul corridors no road journey can substitute); the land-connected subset that AV can target; and what remains after the AVcore shift. The first gap is the airport's geographically non-addressable flying, the second is the switching. The addressable share varies sharply: mainland hubs and gateways (Amsterdam, the German and Iberian airports) carry a majority of their personal air on land-connected routes, whereas island gateways (Palma, the Canaries, the Greek islands) carry almost none, so their traffic is untouched by

road substitution however good the car becomes – the same passenger–emissions geography that bounds the aggregate result (Section 5), read airport by airport.

The connection buckets are those defined in Section 4, keyed to the 20 largest airports by personal air passengers, and the feeder pivot is applied with the graded weight introduced there. This matters for near-identical corridors that a hard cut would split: Edinburgh–London Heathrow (observed air 92 %, 31 trains/day) and Glasgow–London Heathrow (84 %) are physically alike, yet a binary suspect cut at 90 % observed air would pivot the first fully and the second not at all – the former then shedding under a fifth of its air, the latter over half. The graded logistic of Eq. (9) instead gives them pivot weights of 0.59 and 0.23 (Glasgow, at 84 % observed air, sits just below the 90 % midpoint yet still eligible), so their responses vary smoothly with the connection signal rather than jumping across a threshold, just as the elasticity ramp of Eq. (6) smooths the drive-time regimes. Grading leaves the headline (24.6 %, 15.1 Mt) and the genuine-route held-out fit essentially unchanged from a binary rule – confirming that the pivot's role is to keep contaminated feeders from distorting the estimates, not to fit the feeders themselves – while removing the near-threshold discontinuity.

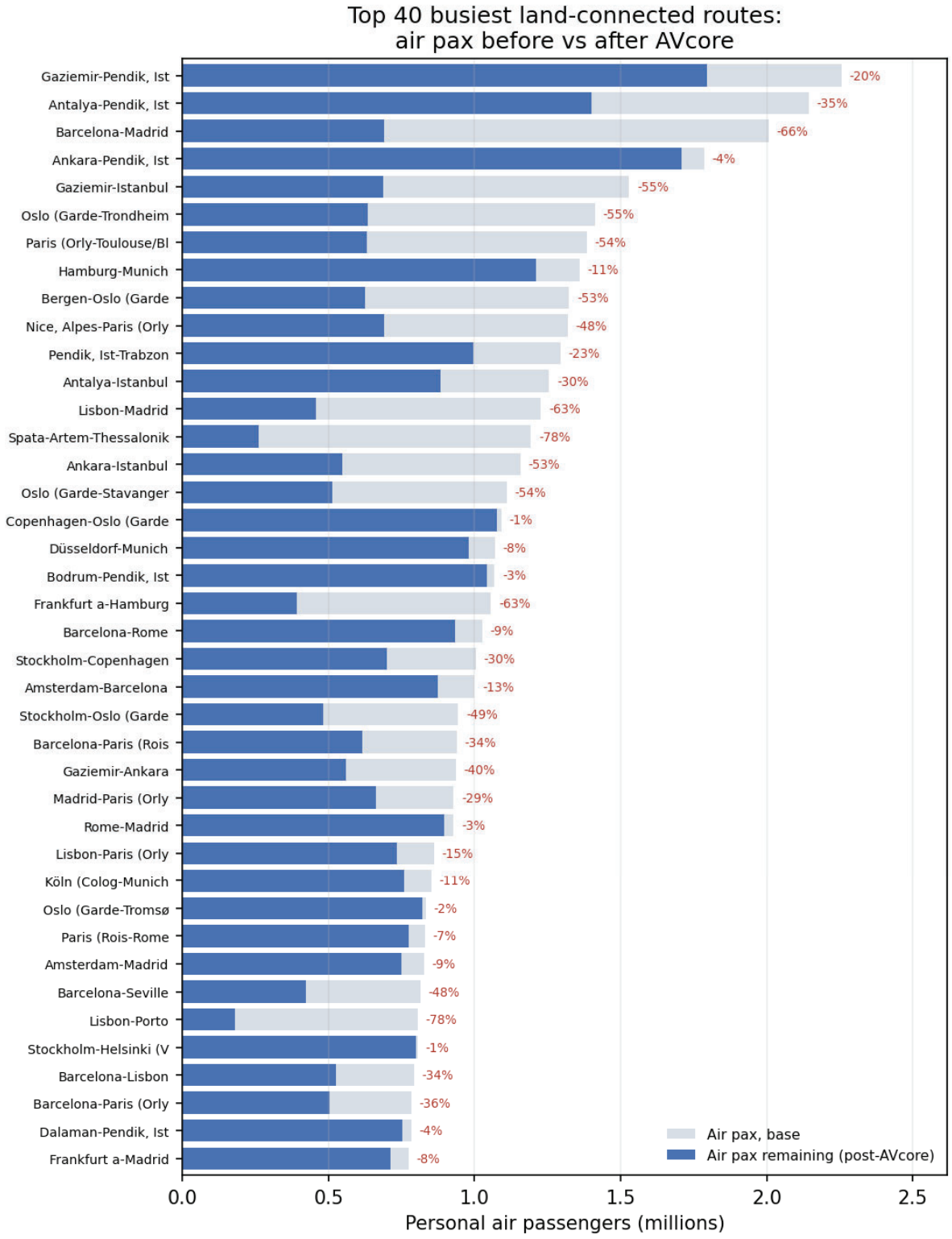


Figure 6: The 40 busiest land-connected routes by personal air passengers, ordered by volume: base air passengers (light) and the post-AVcore remainder (dark); labels give the percentage reduction. Both-hub connection-trunk routes excluded.

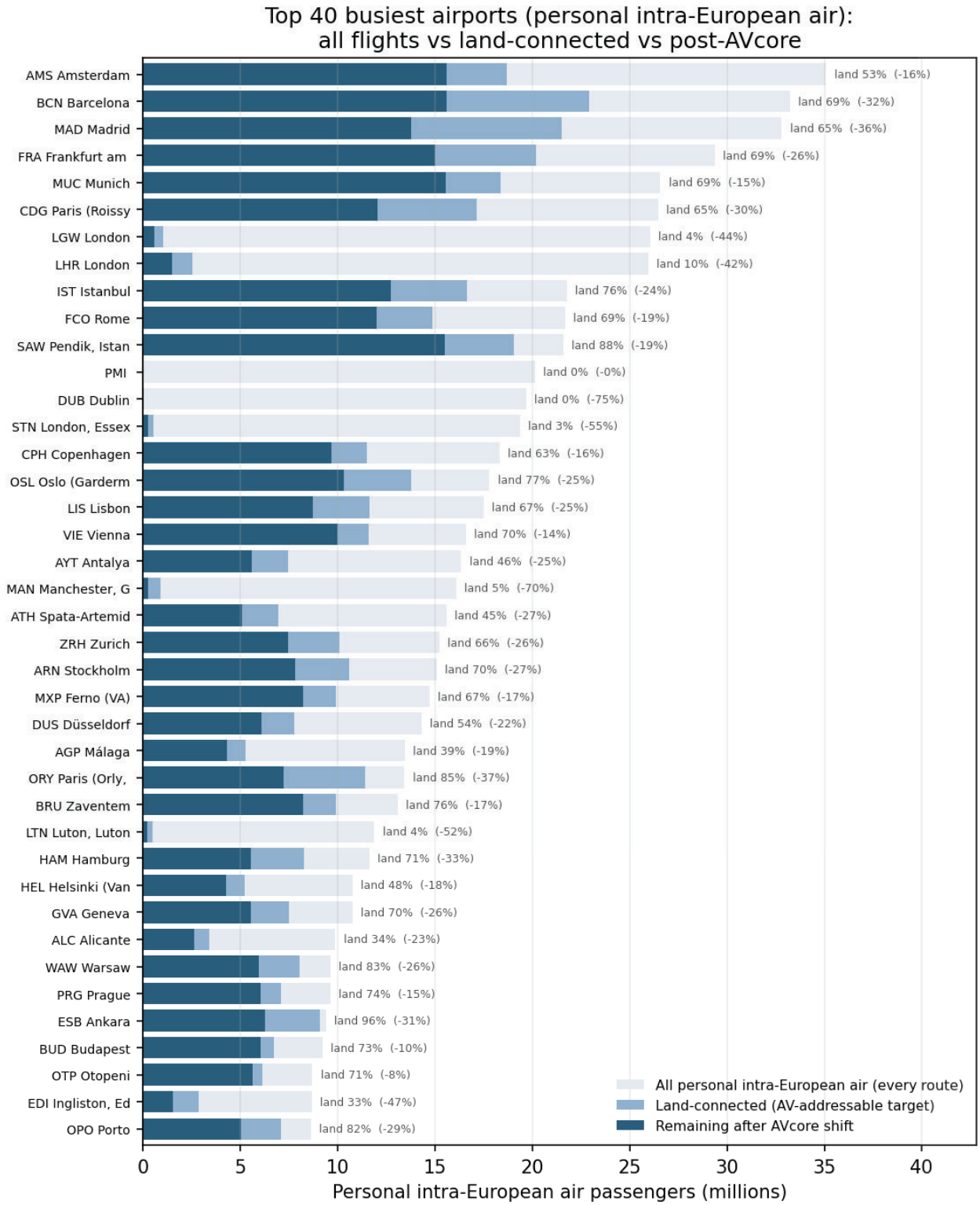


Figure 7: The 40 busiest airports by total personal intra-European air, ordered by volume, in three nested tiers: all personal intra-European air (light), the land-connected AV-addressable subset (mid), and the post-AVcore remainder (dark). Labels give the land-connected share of the airport's air and, in parentheses, the AVcore reduction of that land-connected air.